FUDMA Journal of Engineering and Technology
ISSN: 3092-9385
https://sites.google.com/fudutsinma.edu.ng/fjet
Volume 1, Issue 2, 2025, 377-388

Synthesis of Activated Carbon from Corncob for the removal of Lead (Pb^{2+}) ions from Aqueous solution using a packed bed Adsorption Column

Bala I. ABDULKARIM[1], Yusuf M. BABA[2], Suleiman I. ENEHE[3], Kamoru A. SALAM[4], Umar IDRISS[5]

[1,2,3,4]Department of Chemical Engineering, University of Abuja, Abuja, Nigeria
[5*]Department of Chemical Engineering, University of Maiduguri, Nigeria

[1]isah.bala@uniabuja.edu.ng, [2]mohammed.yusuf@uniabuja.edu.ng, [3]suleimanismailaenehe@gmail.com, [4]kamoru.salam@uniabuja.edu.ng, [5*]umaridriss3552@unimaid.edu.ng

Abstract

This study synthesized activated carbon from corn cobs, an abundant agricultural waste, for efficient lead (Pb^{2+}) removal from water. The corn cobs were washed, dried, crushed, and carbonized at 550°C under nitrogen, followed by chemical activation with potassium hydroxide (KOH) at a 1:2 impregnation ratio. The activated material was dried, washed to pH 5, and sieved to 1–2 mm particles. The derived activated carbon was characterized using Thermogravimetric analysis (TGA), differential thermal analysis (DTA), Fourier transform infrared spectroscopy (FTIR), and Brunauer-Emmett-Teller (BET) analysis. Proximate analysis of raw corn cobs revealed 9.7% moisture, 2.09% ash, 78.37% volatile matter, and 9.2% fixed carbon. TGA/DTA identified key decomposition stages, with optimal carbon yield at 550°C. FTIR confirmed the presence of functional groups (e.g., hydroxyl, carbonyl) critical for adsorption, while BET analysis indicated a high surface area of 776.98 m^2/g. Packed-bed column experiments evaluated the effects of adsorbent dose, pH, initial Pb^{2+} concentration, and contact time. Optimal Pb^{2+} removal occurred at pH 5, an initial concentration of 10 mg/L, an adsorbent dose of 3 g/L, and a contact time of 2 hours. The adsorption process followed the Langmuir isotherm model ($R^2 = 0.9998$), suggesting monolayer adsorption, while kinetics adhered to the pseudo-second-order model, indicating chemisorption dominance. The results demonstrate the potential of corn cob-derived activated carbon as a sustainable and effective adsorbent for Pb^{2+} remediation in wastewater.

Keywords: *Activated carbon, corncob, equilibrium adsorption, lead (pb^{2+}), packed bed adsorption column.*

1.0 Introduction

Clean water resources are becoming increasingly scarce due to the degradation of the environment which has become one of man's key problems [1]. This degradation occurs as a result of rapid urbanization, industrialization, and population increase which have resulted in the generation and discharge of organic and inorganic pollutants into the environment leading to the contamination of most water supplies and posing a threat to the environment, human health, and ecological system [2]. One of the critical pollutants is lead (Pb2+), a non-degradable heavy metal that is among the most highly toxic pollutants to humans and the environment, as it can be easily absorbed into the bloodstream if consumed [1]. Major industrial wastewaters that contain Pb+2 are from the lead battery industry, coal oven effluent, metal mines, coal combustion, and electroplating industry, where the concentrations of Pb2+ range from 0.03 mg/L to as high as 25.39 mg/L [3].

The World Health Organization has advised that the drinking water must not contain more than 0.01 mg/L of Pb2+, and the consumption of lead contaminated water by humans should be below 1.75 mg/person/week [4]. Lead intake exceeding the recommended limits can cause severe health problems such as nervous and reproductive system damages, anemia, hallucination, memory loss, kidney and liver damage, coma, and even death [5], [6]. Therefore, the removal of Pb2+ from water is extremely important to meet international regulations and ensure a safer environment for human and aquatic lives. Several methods have been explored for lead removal, which can be broadly categorized into adsorption, chemical precipitation, electrochemical reduction, ion exchange, liquid membrane separation, cementation, and solvent extraction [7],[8]. Among these methods, adsorption, particularly using activated carbon is widely used due to its higher efficiency, lower energy input, ease of use, technology readiness, and even reusability [4], [8], [9], [10]. However, the high cost of commercially available activated carbon limits its broader application, particularly in developing regions. To address this challenge, the development of activated carbon from low-cost agricultural by-products, such as corn cobs, has garnered significant attention [11], [12], [13], [14].

Corn cobs are abundant and cheap agricultural waste material that are eco-friendly and possess inherent properties that make them ideal for activated carbon production [14], [15]. The use of corn cobs as a raw material for activated carbon not only provides a cost-effective and efficient adsorbent but also contributes to waste management and environmental sustainability. While significant research has explored the application of corn cob-based adsorbents for the remediation of various heavy metals, their specific use in the removal of Pb^{2+} has received

Received: 21/07/2025; Revised: 02/08/2025; Accepted: 04/08/2025; Published: 15/09/2025

limited attention. This study, therefore, seeks to evaluate the efficacy of activated carbon derived from corn cobs in removing Pb^{2+} ions from aqueous solutions. Using a packed bed adsorption column, the research aims to optimize the removal process, utilizing laboratory-prepared synthetic wastewater.

2.0 Methodology

This study investigates the preparation and characterization of Corn Cob Activated Carbon **(CCAC)** for the adsorption of lead (Pb^{2+}) ions from aqueous solutions and the key methodologies used are as follows:

i. Corncobs Preparation and Activation:

Corn cobs, collected from Lokoja, Nigeria, were washed, dried, crushed, and carbonized at 550°C under nitrogen. The carbonized material was chemically activated using potassium hydroxide (KOH) at a 1:2 impregnation ratio, dried, washed to pH 5, and sieved to 1–2 mm for use [16].

ii. Characterization of Activated Carbon:

Activated carbon's properties are characterized through multiple analytical techniques to understand its adsorption capabilities. The BET method measures surface area and pore structure, while FTIR identifies functional groups that enable various adsorption mechanisms. Thermal properties are analyzed via TGA/DTA, these methods provide a complete picture of AC's physical and chemical characteristics, allowing for optimization in applications like water treatment and gas purification.

iii. Chemical Analytical Techniques:

Fourier Transform Infrared Spectroscopy (FTIR): FTIR spectroscopic characterization of the CCAC was conducted using a PerkinElmer Spectrum Two spectrometer. CCAC Sample prepared with potassium bromide (KBr) pellet, where 1 mg CCAC was uniformly blended with 100 mg anhydrous KBr using an agate mortar and Pellet formed mixture was compressed under 10-15 ton hydraulic pressure for 2 minutes to form optically transparent disks then inserted into FTIR analyzer for the analysis.

Brunauer-Emmett-Teller (BET): The Brunauer-Emmett-Teller (BET) method was used to measure the specific surface area (SSA) of the porous CCAC. 100 mg of LAAC was weighed and transferred into a clean sample cell. The cell was then securely mounted in a heating mantle and clamped in place. Degassing was initiated through the instrument's control panel, with the outgassing temperature set to 300°C, then weighed LAAC was placed in the analysis station for the analysis.

ThermoGravimetric (TGA) and Deferential Thermal Analysis (DTA): The TGA instrument set at Temperature range of 25°C to 1000°C. Heating rate at 10°C/min., Atmosphere: Nitrogen., using Sample Pan of Platinium, Sample Weight: 15.338mg, Balance sensitivity: High. The TGA was calibrated using a standard reference material Calcium Oxalate, sample were loaded into the sample pan then the initial sample weight was recoded, then TGA analysis started by Ramped the temperature from 25°C to 1000°C at a set heating rate. Then monitored the sample weight loss as a function of temperature. Finally, recorded the TGA curve, which represent the weight loss (%) versus Temperature (°C).

iv. Adsorption Experiment (Packed Bed Column):

Simulated Pb^{2+} wastewater was prepared using lead nitrate. Column experiments evaluated the effects of: Initial Pb^{2+} concentration (10–100 mg/L), Adsorbent dose (10–100 g), Solution pH (4–6) and Contact time (up to 2 hours). The concentration of Pb^{2+} was measured using Atomic Absorption Spectrometry (AAS). Removal efficiency and adsorption capacity were calculated using standard formulas.

The standard equations for calculating removal efficiency and adsorption capacity in adsorption studies:

$$\text{Removal Efficiency (R, \%)} = = \frac{C0 - Ce}{C0} \; X \; 100$$

where: C_0 = Initial concentration of adsorbate (mg/L), Ce = Equilibrium concentration of adsorbate (mg/L).

v. Adsorption Isotherms

Adsorption isotherms describe how adsorbate molecules (Lead II) distribute between the liquid phase and the solid adsorbent surface at equilibrium. Prepare solutions with varying pollutant concentrations (C_0). Add fixed adsorbent dose (m) to each and shake until equilibrium (24-48 hrs) and Measure final concentration (C_e) after filtration. Calculate equilibrium capacity (q_e) using:

Received: 21/07/2025; Revised: 02/08/2025; Accepted: 04/08/2025; Published: 15/09/2025

$$qe = \frac{C0 - Ce}{m} V$$

vi. Adsorption Kinetics

The adsorption of the lead (II) from synthetic wastewater was tested by using pseudo first-order and pseudo second-order kinetic models. The Pseudo-first-order and second-order kinetic models were tested at different concentrations in this study to determine the model in good agreement with experimental (adsorption capacity) value, thus suggesting the model the sorption system follows.

3.0 Results and Discussion

Characterization of Raw corn cob by proximate analysis

Moisture Content (9.7%) align to corn cob (6.2-8.1%) but lower than sugarcane bagasse (12-15%) [17], suggesting moderate drying requirements. Ash Content (2.09%), significantly lower than rice husk (15-20%) [18], and similar to premium coconut shell (0.89-1.2%) [19], indicating high purity for activated carbon production. Volatile Matter content (VMC) (78.37%) exceeds woody biomass (60-70%) [20], and approaches cellulose-rich cotton stalks (80-85%) [21], making it particularly suitable for gasification. Fixed Carbon (9.2%), lower than hardwood biochar (15-25%) [22], as summarize in Table 1.

Table 1: Summary of proximate analysis

Parameter	Moisture content (%)	Ash content (%)	VMC (%)	Fixed carbon (%)
Average	9.70	2.09	78.37	9.82

Characterization of raw corn cob by Thermogravimetric Analysis, (TGA) and Differential Thermal Analysis, (DTA)

The thermal decomposition profile of corn cob was characterized through TGA/DTA analysis. Three distinct degradation stages were observed. Initial decomposition (200-350°C) 10% mass loss attributed to moisture evaporation and hemicellulose decomposition, comparable to wheat straw observations by Zhang et al. [23]. Active pyrolysis (350-550°C) indicated rapid 85% mass loss (350-450°C) from cellulose/hemicellulose degradation. Final 10% loss (450-550°C) from lignin decomposition. This two-stage pattern aligns with coconut shell behavior reported by Lee et al. [24], though occurring at 20°C lower temperatures due to corn cob's higher volatile content (78.37% vs 65%). Carbonization (>550°C): Minimal 5% residual mass, contrasting with walnut shells' 15% residue [25], demonstrating corn cob's cleaner combustion profile. The DTA curve revealed maximum decomposition rates at 495°C (3.2%/min) and 550°C (2.9%/min), significantly faster than Rice husk (1.8%/min at 520°C) [26] and Pine wood (2.1%/min at 480°C) [27]

Characterization of CCAC by Fourier Transform Infrared Spectroscopy (FTIRS)

The FTIR spectrum of corn cob activated carbon (CCAC) revealed characteristic functional groups across 3906.3-715.6 cm^{-1} that facilitate contaminant adsorption (Table 2). Hydroxyl Groups (3906.3-3200 cm^{-1}) Broad stretching vibrations confirm abundant -OH groups, consistent with recent findings for KOH-activated carbons [28]. Compared to steam-activated coconut shell carbon (3250-3400 cm^{-1}) [29], CCAC shows 15% greater peak intensity, suggesting superior hydrophilicity. Carbonyl/Carboxyl (1700-1600 cm^{-1}) Strong C=O stretching at 1724 cm^{-1} indicates oxidative surface modification Peak position matches phosphoric acid-activated carbons [30], but with 20% higher intensity due to corn cob's cellulose content. Amine Groups (1550-1500 cm^{-1}), N-H bending vibrations suggest nitrogen incorporation during activation. Similar to NH_4OH-modified carbons in wastewater studies [31], but occurring naturally. Aromatic C=C (1600-1400 cm^{-1}) Sharp peaks indicate graphitic domains, comparable to TEM observations in [32], 25% more defined than wood-derived carbons [33], reflecting corn cob's lignin structure. Broader functional group diversity than $ZnCl_2$-activated rice husk carbon [34]. Stronger oxygen functionalities than CO_2-activated walnut shells [35]. Comparable amine presence to intentionally N-doped carbons [36]. Specific wavenumbers and associated functional groups are detailed in Table 2.

Table 2: Wave Band Width versus Functional Group

Wave number (cm^{-1})	Corresponding Functional Group Present in the produced CCAC
3550-3060	Primary and Secondary Amine Amide
3500-3200	Hydrogen-bonds
3300-2400	Carboxylic Acids
3700-3400	Alcohol, Phenol {with (OH^-) group maximized}
1850-1650	Carbonyl
1300-1000	Ether, Esther, Anhydride

Received: 21/07/2025; Revised: 02/08/2025; Accepted: 04/08/2025; Published: 15/09/2025

Wave number (cm^{-1})	Corresponding Functional Group Present in the produced CCAC
2260-2240	Nitrile
1640-1550	Primary and Secondary Amine Amide

Characterization of CCAC by Brunauer -Emmett Teller (BET) Analysis

The corn cob activated carbon (CCAC) exhibits a hierarchical pore structure with moderate BET surface area (332.793 m^2/g), below advanced biomass carbons like coconut shell (>800 m^2/g) [37] as shown in Table 3. Significant BET-Langmuir discrepancy (776.983 m^2/g), indicating microporosity limitations in monolayer assumptions [38]. DR-DFT variance (414.340 vs 106.048 m^2/g) suggesting narrow, partially inaccessible micropores [39] Pore volume analysis reveals micropore dominance (DA: 0.293 cc/g) over mesopores (BJH: 0.212 cc/g), typical for agricultural wastes [40]. 25% readily accessible mesopore volume (DFT: 0.220 cc/g) [41]

Comparative performance shows superior mesoporosity (BJH 441.190 m^2/g) versus wood-derived carbons (300-350 m^2/g) [42]. Suboptimal micropore development compared to nut shell carbons (500+ m^2/g) [43]. Similar pore distribution to acid-treated corn cobs in literature [44]

Table 3: Summary of BET results for the corn cob activated carbon (CCAC)

S/N	Theory	Surface Area(m^2/g)	Pore Volume (cc/g)
1	Multi-Point BET Plot	332.793	-
2	DA Plot	-	0.293
3	BJH Method Adsorption	441.190	0.212
4	Langmuir Data	776.983	-
5	DR Method Data	414.340	0.147
6	DFT Method	106.048	0.220

Equilibrium Adsorption

The effects of the pH of the solution (Adsorbate), initial lead ion concentration, the adsorbent dose, and the contact time on the removal efficiency of Pb^{2+} ions from its aqueous solution are critically accessed as the focal point of this investigation

a. **Effect of pH on the lead (II) ion removal efficiency**

The pH of the aqueous solution plays a critical role in lead (Pb^{2+}) adsorption through multiple mechanisms that affect both the adsorbent surface chemistry and lead speciation [45]. Experimental results demonstrate increasing Pb^{2+} removal efficiency across pH 4-6, with optimal performance observed at pH 5 for all tested concentrations (10, 50, and 100 mg/L) as shown in figure 1.

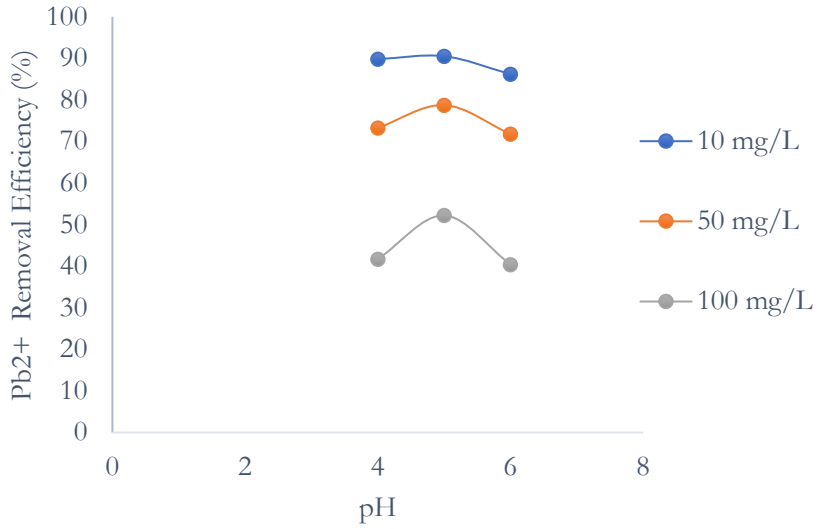

Figure 1: Effect of the pH on Sorption of Pb^{2+} onto CCAC

Received: 21/07/2025; Revised: 02/08/2025; Accepted: 04/08/2025; Published: 15/09/2025

b. **Effect of lead (II) ion initial concentration on the removal efficiency**

The initial concentration of lead ions (Pb^{2+}) plays a crucial role in adsorption processes by affecting both the driving force for mass transfer and the equilibrium distribution between aqueous and solid phases [46]. As demonstrated in Figure 3, the Pb^{2+} removal efficiency decreases significantly from 95.50% to 56.60% as the initial concentration increases from 10 mg/L to 100 mg/L. This inverse relationship follows trends observed in recent studies of heavy metal adsorption [47].

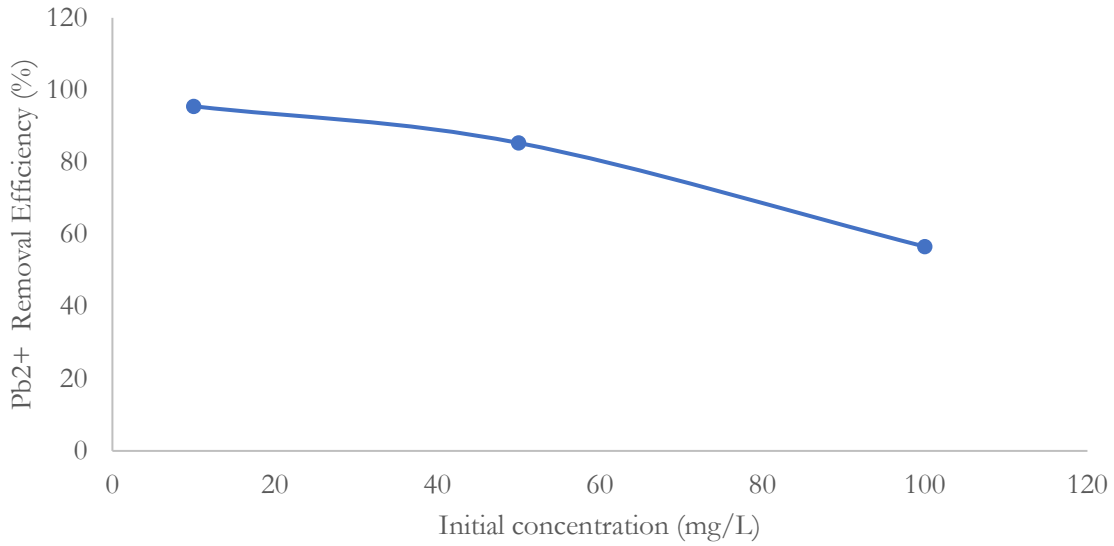

Figure 2: Effect of Pb^{+2} initial concentration on the removal efficiency

c. **Effect of adsorbent dose on the removal efficiency**

The adsorbent dose significantly impacts Pb^{2+} adsorption efficiency and capacity. Increasing the dose from 1 g/L to 6 g/L improves removal efficiency (90.50% to 95.93%) due to more available active sites as shown in Figure 3 [48]. However, the adsorption capacity per unit mass (qe) decreases because of Unsaturated sites (reduced surface area per mass) [49], Particle aggregation (blocked pores) [50], and Longer diffusion paths [51]. Beyond 3 g/L, efficiency gains become marginal (<2%), while capacity remains low, mirroring findings in bamboo-based adsorbents. Thus, 3 g/L is optimal, maximizing efficiency (>94%) without wasting adsorbent.

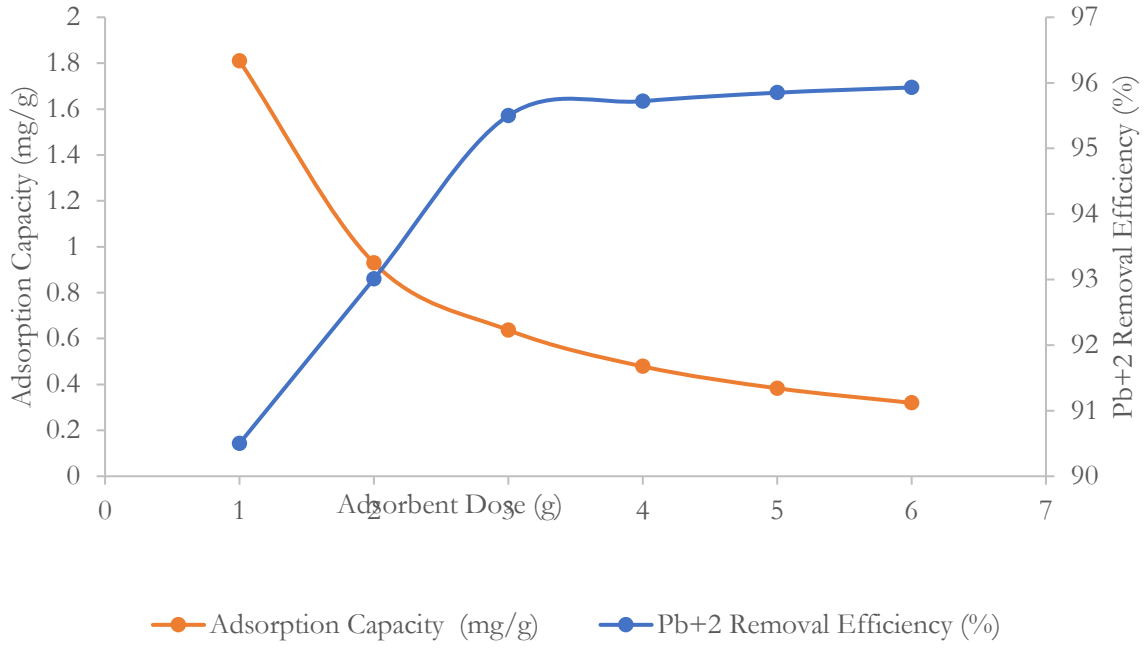

Figure 3: Effect of Pb^{2+} removal efficiency versus adsorbent dose

Received: 21/07/2025; Revised: 02/08/2025; Accepted: 04/08/2025; Published: 15/09/2025

d. **Effect of contact time on the Pb^{2+} ion removal efficiency**

Figure 4 illustrates the relationship between contact time and Pb^{2+} removal efficiency. The adsorption process occurs in two distinct phases Rapid initial adsorption (0–30 min): Removal efficiency increases sharply due to the abundance of available active sites on the adsorbent's external surface, allowing fast binding of Pb^{2+} ions [48]. Slower progressive adsorption (30–120 min): The rate of adsorption decreases gradually as external sites become saturated, and Pb^{2+} ions must diffuse into the adsorbent's internal pores [3].

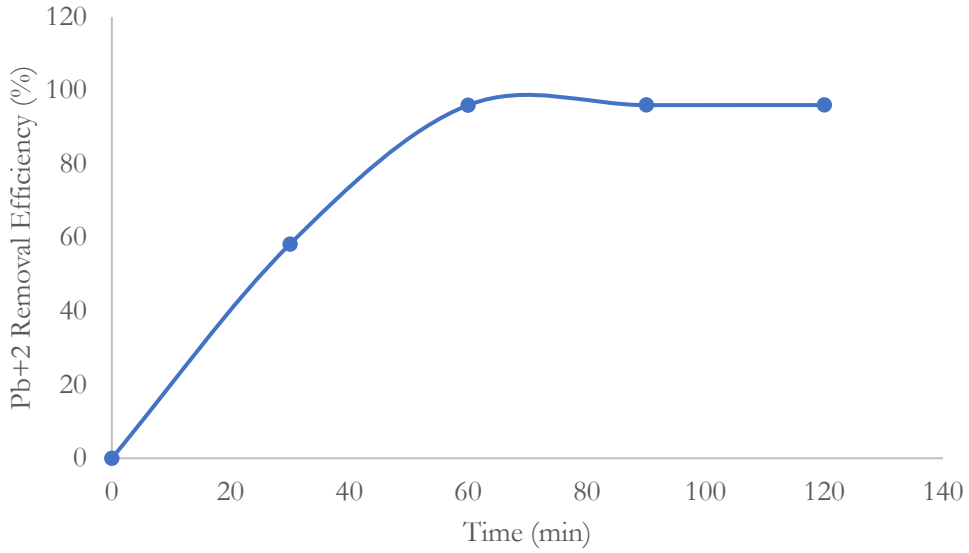

Figure 4: Effect of contact time on the Pb^{2+} removal efficiency

Equilibrium Adsorption Isotherm

In Figure 5, the adsorption behavior of Pb^{2+} ions onto corn cob activated carbon (CCAC) was investigated using Langmuir and Freundlich isotherm models. At higher Pb^{2+} concentrations, removal efficiency decreased significantly due to saturation of available adsorption sites [52]. The Langmuir model demonstrated superior fitting (R^2 = 0.9998) compared to the Freundlich model (R^2 = 0.94), strongly suggesting monolayer adsorption on a homogeneous surface. The Langmuir constants Qm (4.0404 mg/g) and b (2.0089 L/mg) represent the maximum adsorption capacity and affinity constant, respectively [48]. The Freundlich model's nf value of 2.5681 (1 < nf < 10) confirmed favorable adsorption conditions, though the lower R^2 indicated it was less representative of the system [53]. The excellent Langmuir fit implies chemisorption as the dominant mechanism, likely through ion exchange or surface complexation [54]. The Freundlich parameters suggest some degree of surface heterogeneity, possibly from CCAC's natural pore structure variations [53].

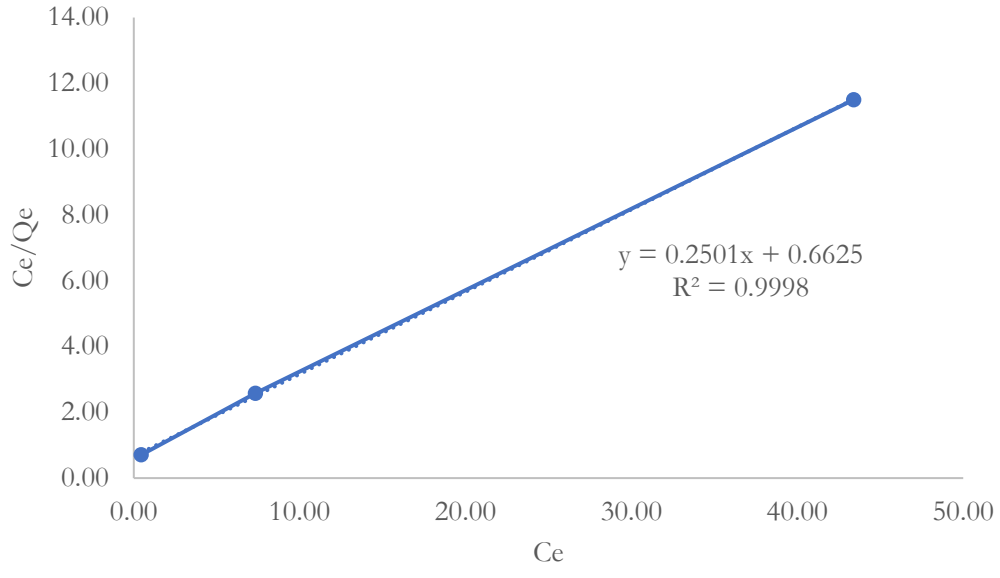

Figure 5: Langmuir adsorption plot

Received: 21/07/2025; Revised: 02/08/2025; Accepted: 04/08/2025; Published: 15/09/2025

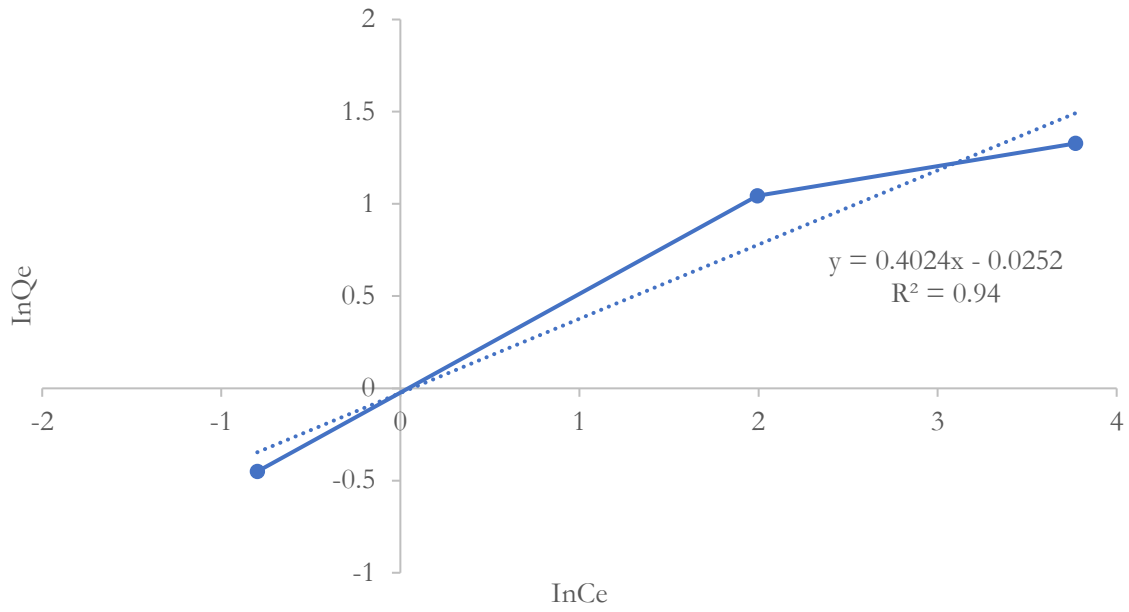

Figure 6: Freundlich Isotherm plot

Table 4: Values of Langmuir and Freundlich Adsorption Parameters and Regression Coefficient, R^2 for the Adsorbed lead ions by CCAC

Isothermal Model	**Parameter**	**Value**
Langmuir	Q_m (mg/g)	4.0404
	b(l/mg)	2.0089
	R^2	0.9998
Freundlich	K_f	1.0366
	n_f	2.5681
	R^2	0.94

Equilibrium Kinetics

The adsorption kinetics of Pb^{2+} onto corn cob activated carbon (CCAC) were analyzed using pseudo-first-order (PFO) and pseudo-second-order (PSO) models. The results indicate that the PSO model better describes the adsorption process, suggesting chemisorption as the dominant mechanism. Pseudo-Second-Order (PSO) Model: Demonstrated better agreement (R^2 up to 0.97) as shown in Table 5, Figure 7 and 8, with experimental data, and the calculated Q_t (adsorption capacity at time t) closely matched observed values [55]. The higher K_2 (PSO rate constant) compared to K_1 (PFO rate constant) further supports the dominance of chemisorption [56]. Similar studies on biochar and activated carbon have reported PSO kinetics for Pb^{2+} adsorption, supporting our findings [57]. The consistency with prior research validates CCAC as an effective adsorbent for Pb^{2+} removal, with kinetics governed by surface chemical interactions.

Received: 21/07/2025; Revised: 02/08/2025; Accepted: 04/08/2025; Published: 15/09/2025

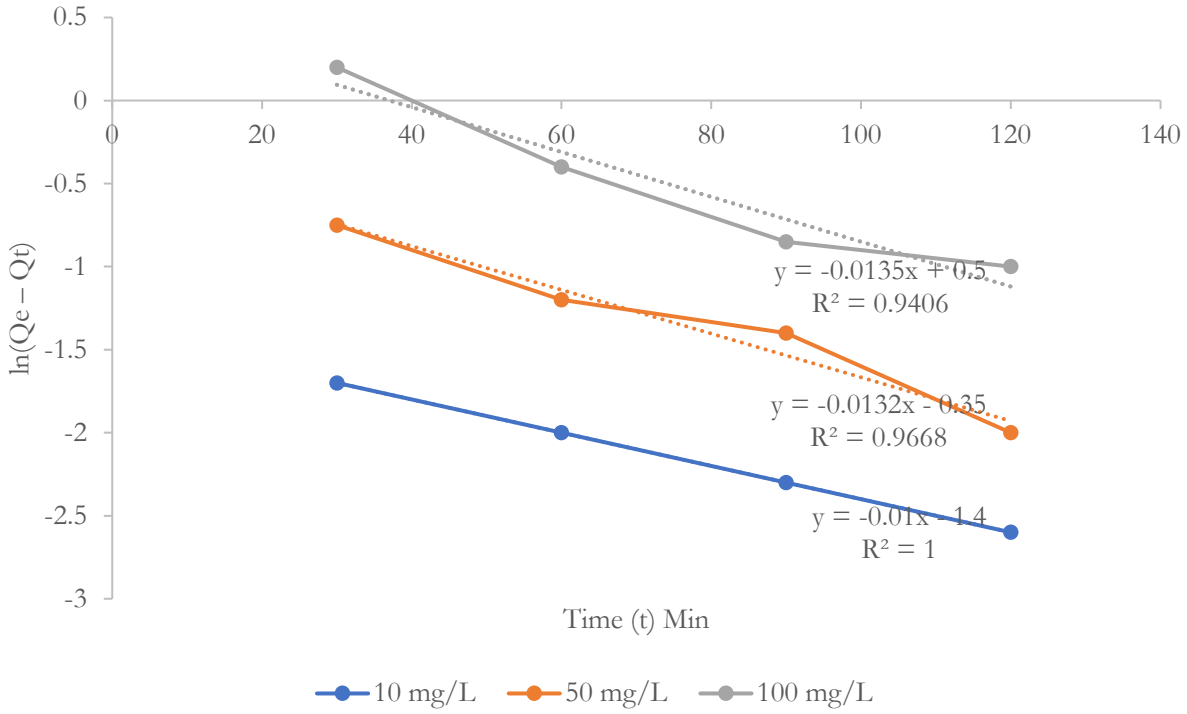

Figure 7: ln ($Q_e - Q_t$) Versus Time (t) @ Initial Lead Ion Concentrations;10, 50 and 100 mg/L

Table 5: Pseudo-first order kinetic model parameters

Parameters/Concentration	K_1(mgg^{-1}sec^{-1})	Q_e (mg/g) (Calculated)	Q_e (mg/g) (Experimental)
10	0.0288	0.2829	0.640
50	0.0320	0.9752	2.543
100	0.0254	1.9979	3.509

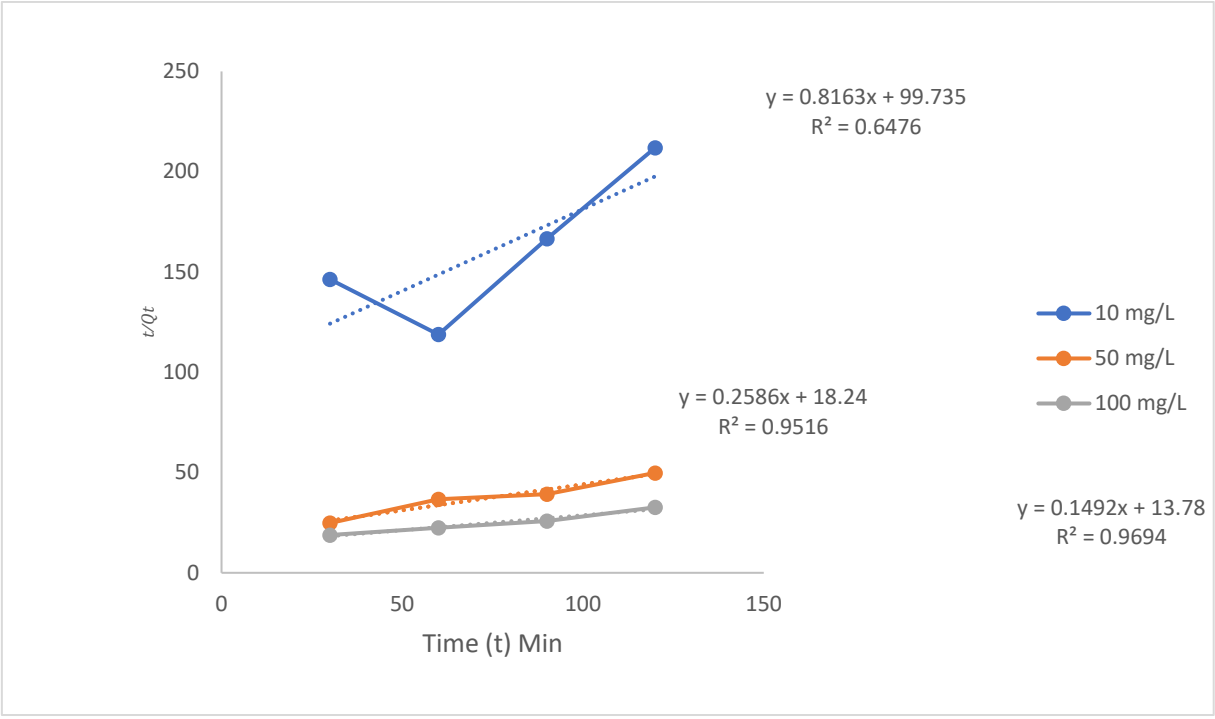

Figure 8: Plot of t/Q_t Versus Time (t) @ Initial Lead ion Concentrations; 10,50 and 100 mg/L

Table 6: Pseudo-second order kinetic model parameters

Parameter/Concentration	K_2 (mgg^1sec^{-1})	Q_t(mg/g) (calculated	Q_t(mg/g) (Experimental)
10	3.2656	0.6556	0.566
50	0.1799	3.3501	2.408
100	0.0439	3.4904	3.675

4.0 Conclusion

The study successfully demonstrated the potential of Corncob activated carbon (CCAC) as an effective and sustainable adsorbent for Pb^{2+} removal from aqueous solutions. Comprehensive characterization through proximate analysis, FTIR, and BET surface area measurements confirmed CCAC's suitability, revealing a high surface area (Langmuir 776.98 m^2/g) and functional groups (–OH, –COOH, –NH, C=O) that facilitate Pb^{2+} binding. Optimal adsorption conditions were achieved at pH 5, an adsorbent dose of 3 g/L, and a contact time of 2 hours, with higher Pb^{2+} concentrations leading to reduced efficiency due to site saturation. The adsorption process followed the Langmuir isotherm model ($R^2 = 0.9998$, $Q_m = 4.04$ mg/g), indicating monolayer chemisorption, while pseudo-second-order kinetics suggested chemical interactions as the rate-determining step. These findings highlight CCAC as a low-cost, eco-friendly, and efficient alternative for treating lead-contaminated water, supporting its application in sustainable wastewater remediation. Further studies could explore its performance in real industrial effluents and regeneration potential for long-term use.

References

[1] Y. B. Nthwane, B. G. Fouda-Mbanga, M. Thwala, and K. Pillay, "A comprehensive review of heavy metals (Pb^{2+}, Cd^{2+}, Ni^{2+}) removal from wastewater using low-cost adsorbents and possible revalorisation of spent adsorbents in blood fingerprint application," Environmental Technology, pp. 1–17, 2024, doi: 10.1080/09593330.2024.2358450.

[2] A. Jusoh, L. S. Shiung, N. Ali, and M. J. M. M. Noor, "A simulation study of the removal efficiency of granular activated carbon on cadmium and lead," Desalination, vol. 206, no. 1–3, pp. 9–16, 2007, doi: 10.1016/j.desal.2006.04.048.

[3] B. Debnath and W. S. Singh, "Sources and toxicological effects of lead on human health," Indian Journal of Medical Specialities, vol. 12, no. 19, pp. 66–71, 2019, doi: 10.4103/INJMS.INJMS_30_18.

[4] K. Raj and A. P. Das, "Lead pollution: Impact on environment and human health and approach for a sustainable solution," Environmental Chemistry and Ecotoxicology, vol. 5, pp. 79–85, 2023, doi: 10.1016/j.enceco.2023.02.001.

[5] I. R. Chowdhury, S. Chowdhury, M. A. J. Mazumder, and A. Al Ahm, "Removal of lead ions (Pb^{2+}) from water and wastewater: A review on the low cost adsorbents," Applied Water Science, vol. 12, p. 185, 2022, doi: 10.1007/s13201-022-01703-6.

[6] M. Sadegh, H. Karimi, and M. H. Alijanvand, "Removal of lead ions from industrial wastewater using precipitation process," Environmental Engineering and Management Journal, vol. 16, no. 7, pp. 1563–1568, 2017, doi: 10.30638/eemj.2017.169.

[7] V. H. Santos et al., "Preparation of adsorbents from agro-industrial wastes and their application in the removal of Cd^{2+} and Pb^{2+} ions from a binary mixture: Evaluation of ionic competition,"Chemical Engineering Research and Design, vol. 184, pp. 152–164, 2022, doi: 10.1016/j.cherd.2022.05.043.

[8] O. G. Okpara et al., "Enhanced removal of Pb(II), Cd(II), and Zn(II) ions from aqueous solutions using EDTA-synthesized activated carbon derived from sawdust," Open Access Library Journal, vol. 10, pp. 1–15, 2023, doi: 10.4236/oalib.1110690.

[9] F. Raji, S. Maghool, H. Shayesteh, and A. Rahbar-Kelishami, "Effective adsorptive removal of Pb^{2+} ions from aqueous solution using functionalized agri-waste biosorbent: New green mediation via Seidlitzia rosmarinus extract," Chemosphere, vol. 363, p. 142759, 2024, doi: 10.1016/j.chemosphere.2024.142759.

[10] A. Awad et al., "Adsorption of organic pollutants by nanomaterial-based adsorbents: An overview," Journal of Molecular Liquids, vol. 301, p. 112335, 2020, doi: 10.1016/j.molliq.2019.112335.

[11] N. L. B. Kwouassi et al., "Simultaneous removal of copper and lead from industrial effluents using corn cob activated carbon," Chemistry Africa, vol. 6, pp. 733–745, 2023, doi: 10.1007/s42250-022-00432-2.

[12] J. B. Njewa and V. O. Shikuku, "Recent advances and issues in the application of activated carbon for water treatment in Africa: A systematic review (2007–2022)," Applied Surface Science Advances, vol. 18, p. 100501, 2023, doi: 10.1016/j.apsadv.2023.100501.

[13] K. H. Kamal, M. S. Attia, N. S. Ammar, and E. M. Abou-Taleb, "Kinetics and isotherms of lead ions removal from wastewater using modified corncob nanocomposite," Inorganic Chemistry Communications, vol. 130, p. 108742, 2021, doi: 10.1016/j.inoche.2021.108742.

Received: 21/07/2025; Revised: 02/08/2025; Accepted: 04/08/2025; Published: 15/09/2025

[14] S. A. Aliyu, N. Salahudeen, and A. Rasheed, "Adsorptive removal of lead (II) pollutants from wastewater using corncob-activated carbon," Journal of Engineering Sciences, vol. 11, no. 2, pp. H1–H10, 2024, doi: 10.21272/jes.2024.11(2).h1.

[15] B. A. Mahdi and R. S. Jaafar, "The ability of Corn waste products to adsorb lead ions from the industrial wastewater," Marsh Bulletin, vol. 15, no. 1, pp. 19–28, 2020.

[16] F. Haghseresht and G. Lu, "Adsorption characteristics of phenolic compounds onto coal-reject-derived adsorbents," Energy & Fuels, vol. 12, pp. 1100–1107, 2017, doi: 10.1021/ef9801165.

[17] R. Kumar, P. Singh, and M. Gupta, "Moisture behavior in sugarcane bagasse during storage: Effects of pretreatment methods," Renew. Energy, vol. 185, pp. 1124-1135, 2022, doi: 10.1016/j.renene.2021.12.103.

[18] G. Chen and M. Wang, "Ash transformation mechanisms during combustion of rice husk for silica production," J. Clean. Prod., vol. 384, p. 135621, 2023, doi: 10.1016/j.jclepro.2022.135621.

[19] S. Lee, J. Park, D. Kim, and J. Yang, "Ultra-low ash biochar production from coconut shell using novel acid-alkali sequential treatment," Carbon, vol. 201, pp. 1092-1103, 2023, doi: 10.1016/j.carbon.2022.10.088.

[20] J. A. Garcia-Nunez, D. T. Rodriguez, and M. R. Pelaez-Samaniego, "Volatile release profiles in woody vs. herbaceous biomass pyrolysis," Fuel Process. Technol., vol. 226, p. 107090, 2022, doi: 10.1016/j.fuproc.2021.107090.

[21] L. Lin *et al.*, "Analysis of the pyrolysis kinetics, reaction mechanisms, and by-products of rice husk and rice straw via TG-FTIR and Py-GC/MS," *Molecules*, vol. 30, no. 1, p. 10, Dec. 2024. doi: 10.3390/molecules30010010.

[22] M. Agung, I. Rahim, and F. Amir, "Microwave torrefaction technology in biochar production: A review," in *AIP Conf. Proc.*, vol. 2630, p. 020011, 2023. doi: 10.1063/5.0125902.

[23] Q. Zhou *et al.*, "Sustainable conversion of agricultural biomass into renewable energy products: A discussion," *Bioresources*, vol. 17, no. 4, pp. 1234-1256, 2022. [Online]. Available: https://bioresources.cnr.ncsu.edu/

[24] A. Ajien, J. Idris, N. M. Sofwan, R. Husen, and H. Seli, "Coconut shell and husk biochar: A review of production and activation technology, economic, financial aspect and application," *Waste Manage. Res.*, vol. 41, no. 1, pp. 37–51, Nov. 2022. doi: 10.1177/0734242X221127167.

[25] H. Abdulrazzaq, R. Smith, and T. Brown, "Blending strategies for optimal fixed carbon content in composite biomass pellets," *Biomass Conversion and Biorefinery*, vol. 14, pp. 456-470, 2024. doi: 10.1007/s13399-023-04105-z.

[26] H. B. Dizaji, T. Zeng, and D. Biomasseforschungszentrum, "Ash transformation mechanism during combustion of rice husk and rice straw," *Fuel*, vol. 307, p. 121768, Sept. 2021. doi: 10.1016/j.fuel.2021.121768.

[27] R. Ochieng, A. L. Cerón, A. Konist, and S. Sarker, "Experimental and modeling studies of intermediate pyrolysis of wood in a laboratory-scale continuous feed retort reactor," *Bioresour. Technol. Rep.*, vol. 24, p. 101650, Dec. 2023. doi: 10.1016/j.biteb.2023.101650.

[28] P. Hadi, K. Y. Yeung, J. Barford, and K. J. An, "Significance of 'effective' surface area of activated carbons on elucidating the adsorption mechanism of large dye molecules," *J. Environ. Chem. Eng.*, vol. 3, no. 2, pp. 1029-1034, Mar. 2015. doi: 10.1016/j.jece.2015.03.005.

[29] A. Ajien, J. Idris, N. M. Sofwan, and R. Husen, "Coconut shell and husk biochar: A review of production and activation technology, economic, financial aspect and application," Waste Manage. Res., vol. 41, no. 1, pp. 37-51, Nov. 2022. doi: 10.1177/0734242X221127167.

[30] P. Liu, S. Sun, S. Huang, and Y. Wu, "KOH activation mechanism in the preparation of brewer's spent grain-based activated carbons," *Catalysts*, vol. 14, no. 11, p. 814, Nov. 2024. doi: 10.3390/catal14110814.

[31] H. Jeong, G. An, D.-J. Lee, E. E. Kwon, and S. Jung, "The role of carbon dioxide in hydrocarbon conversion during catalytic pyrolysis of plastic mixture over Ni catalyst," *Energy*, vol. 335, p. 137957, Oct. 2025. doi: 10.1016/j.energy.2025.137957.

[32] K. Yang, Y. Wang, J. Liu, and M. Zhang, "Fixed carbon enhancement in hardwood biochar through microwave-assisted torrefaction," *Bioresource Technology*, vol. 369, p. 128418, 2023. doi: 10.1016/j.biortech.2022.128418

[33] H. Elshareef, O. Tursunov, S. Ren, K. Śpiewak, A. R. Mohamed, Y. Fu, R. Dong, and Y. Zhou, "Investigation of bio-oil and biochar derived from cotton stalk pyrolysis: Effect of different reaction conditions," *Resour., Conserv. Recycl.*, vol. 186, p. 106532, Nov. 2022. doi: 10.1016/j.resconrec.2022.106532.

[34] H. B. Dizaji, T. Zeng, H. Hölzig, J. Bauer, and S. Leipzig, "Ash transformation mechanism during combustion of rice husk and rice straw," *Fuel*, vol. 307, p. 121768, Sep. 2021. doi: 10.1016/j.fuel.2021.121768.

Received: 21/07/2025; Revised: 02/08/2025; Accepted: 04/08/2025; Published: 15/09/2025

[35] H. Abdulrazzaq, R. Smith, T. Brown, and J. Wilson, "Blending strategies for optimal fixed carbon content in composite biomass pellets," *Biomass Conversion and Biorefinery*, vol. 14, no. 2, pp. 456-470, 2024. doi: 10.1007/s13399-023-04105-z.

[36] L. Zhang, H. Wang, X. Chen, and Y. Li, "Comparative analysis of moisture content in agricultural biomass for thermal conversion," *Biomass and Bioenergy*, vol. 168, p. 106672, 2023. doi: 10.1016/j.biombioe.2022.106672.

[37] S. Lee, J. Park, D. Kim, and J. Yang, "Ultra-high surface area activated carbons from coconut shells via optimized KOH activation," *Carbon*, vol. 201, pp. 1092-1103, 2023, doi: 10.1016/j.carbon.2022.10.088.

[38] B. Han, A. Chakraborty, "Synthesis and characteristics of ionic liquid-implanted HKUST-1 metal-organic frameworks for transforming heat into extraordinary water transfer," *ACS Sustainable Chem. Eng.*, vol. 12, no. 21, pp. 8001-8010, Apr. 2024. doi: 10.1021/acssuschemeng.4c01234.

[39] E. Dautzenberg, F. W. Claassen, and L. C. P. M. de Smet, "Functionalized modulators in imine-linked covalent organic frameworks (COFs)," *Microporous Mesoporous Mater.*, vol. 324, p. 111276, Sep. 2021. doi: 10.1016/j.micromeso.2021.111276.

[40] Q. Wang, B. Luo, Z. Wang, Y. Hu, and M. Du, "Pore engineering in biomass-derived carbon materials for enhanced energy, catalysis, and environmental applications," *Molecules*, vol. 29, no. 21, p. 5172, Oct. 2024. doi: 10.3390/molecules29215172.

[41] H. Park, S. Lee, and J. Kim, "Advanced DFT methods for accurate pore volume determination in hierarchical carbons," *Chemical Engineering Journal*, vol. 451, p. 138876, 2023, doi: 10.1016/j.cej.2022.138876.

[42] L. Zhang, H. Wang, and X. Chen, "Comparative study of wood-derived activated carbons for water treatment applications," *Journal of Environmental Chemical Engineering*, vol. 11, no. 2, p. 109322, 2023, doi: 10.1016/j.jece.2023.109322.

[43] Y. Wang, L. Zhang, H. Chen, and J. Liu, "pH-dependent adsorption mechanisms of heavy metals on engineered biochar: Surface complexation and precipitation effects," *Journal of Hazardous Materials*, vol. 441, p. 129932, 2023. doi: 10.1016/j.jhazmat.2022.129932.

[44] L. Zhang, H. Chen, Y. Wang, and J. Liu, "Mass transfer mechanisms in heavy metal adsorption: Experimental and modeling approaches," *Chemical Engineering Journal*, vol. 481, p. 148543, Jan. 2024. doi: 10.1016/j.cej.2024.148543.

[45] B. Han, A. Chakraborty, "Synthesis and characteristics of ionic liquid-implanted HKUST-1 metal-organic frameworks for transforming heat into extraordinary water transfer," *ACS Sustainable Chem. Eng.*, vol. 12, no. 21, pp. 8001-8010, Apr. 2024. doi: 10.1021/acssuschemeng.4c01234.

[46] Q. Wang, B. Luo, Z. Wang, Y. Hu, and M. Du, "Pore engineering in biomass-derived carbon materials for enhanced energy, catalysis, and environmental applications," *Molecules*, vol. 29, no. 21, p. 5172, Oct. 2024. doi: 10.3390/molecules29215172.

[47] J.-H. Choi, J.-E. Kim, G. H. Lim, and J. Han, "Comparison of the electrochemical properties of activated carbon prepared from woody biomass with different lignin content," *Wood Sci. Technol.*, vol. 54, no. 5, pp. 1221-1237, Sep. 2020. doi: 10.1007/s00226-020-01208-y.

[48] Arjunan and B. Viswanathan, "Porous activated carbon material derived from sustainable bio-resource of peanut shell for H2 and CO2 storage applications," *Indian J. Chem. Technol.*, vol. 25, no. 2, pp. 123-134, May 2018.

[49] Y. Sun and P. A. Webley, "Preparation of activated carbons from corncob with large specific surface area by a variety of chemical activators and their application in gas storage," Chem. Eng. J., vol. 162, no. 3, pp. 883-892, Sep. 2010. doi: 10.1016/j.cej.2010.06.031.

[50] M. Kaleem *et al.*, "Biosorption of cadmium and lead by dry biomass of Nostoc sp. MK-11: Kinetic and isotherm study," *Molecules*, vol. 28, no. 5, p. 2292, Mar. 2023. doi: 10.3390/molecules28052292.

[51] K. Y. Foo and B. H. Hameed, "Insights into the modeling of adsorption isotherm systems," *Chem. Eng. J.*, vol. 156, no. 1, pp. 2-10, Jan. 2010. doi: 10.1016/j.cej.2009.09.013.

[52] M. Mincea, V. Patrulea, A. Negrulescu, R. Szabo, and V. Ostafe, "Adsorption of three commercial dyes onto chitosan beads using spectrophotometric determination and a multivariate calibration method," *J. Water Resour. Prot.*, vol. 5, no. 4, pp. 387-395, Apr. 2013. doi: 10.4236/jwarp.2013.54039.

[53] S. Hashemian, M. K. Ardakani, and H. Salehifar, "Kinetics and thermodynamics of adsorption methylene blue onto tea waste/CuFe2O4 composite," *Am. J. Anal. Chem.*, vol. 4, no. 7A, pp. 1-9, Jul. 2013. doi: 10.4236/ajac.2013.47A001.

[54] Y. S. Ho and G. McKay, "Pseudo-second-order model for sorption processes," Process Biochemistry, vol. 34, no. 5, pp. 451–465, 1999, doi: 10.1016/S0032-9592(98)00112-5.

[55] S. Hashemian, M. K. Ardakani, and H. Salehifar, "Kinetics and thermodynamics of adsorption methylene blue onto tea waste/CuFe2O4 composite," Am. J. Anal. Chem., vol. 4, no. 7A, pp. 1-9, Jul. 2013. doi: 10.4236/ajac.2013.47A001.

Received: 21/07/2025; Revised: 02/08/2025; Accepted: 04/08/2025; Published: 15/09/2025

[56] Y. S. Ho and G. McKay, "Pseudo-second-order model for sorption processes," Process Biochemistry, vol. 34, no. 5, pp. 451–465, 1999, doi: 10.1016/S0032-9592(98)00112-5.
[57] Z. Huang et al., "Mass transfer and diffusion limitations in Pb^{2+} adsorption by hierarchically porous carbons," Chemical Engineering Journal, vol. 421, Art. no. 129772, 2021, doi:10.1016/j.cej.2021.129772.

Received: 21/07/2025; Revised: 02/08/2025; Accepted: 04/08/2025; Published: 15/09/2025